0026-895X/87/050600-06$02.00/0

MOLECULAR PHARMACOLOGY, 32: 600-605

Propidium Binding to a Ribonuclease-DNA Complex: X-Ray and Fluorescence Studies

MARY McGRATH, DULIO CASCIO, ROGER WILLIAMS, DAVID JOHNSON, MARIE GREENE, and ALEXANDER McPHERSON

Department of Biochemistry, University of California, Riverside, California 92521

Received March 31, 1987; Accepted August 6, 1987

SUMMARY

Propidium iodide, an antitumor compound, was diffused into crystals of a complex between RNase A and deoxytetraadenylate ($dpA)_4$). This complex has four deoxyoligomers bound per protein molecule. A difference Fourier analysis at 2.9 Å showed that the principal binding site for the propidium in the crystals was a hydrophobic depression on the side of RNase away from the active site and apparently involves methionine 13 and phenylalanine 8. Binding of propidium at this site produces small conformational changes that effect binding of nucleotides at the active site of the enzyme. Fluorescence titrations in the presence and absence of nucleotide inhibitors suggested that propidium iodide is a competitive inhibitor of the enzyme with a K_i of approximately 1 mM. No significant binding of propidium to the 16 nucleotides of single-stranded DNA associated with each protein molecule was observed.

Propidium iodide (Fig. 1) is a phenanthrene derivative that exhibits significant antitumor and anti-trypanocide activity (1). Although it is known to bind to DNA in an intercalative manner (2), the mechanism by which it kills cells remains in question. For example, brominated derivatives of some related drugs are nonintercalating but still cytotoxic (3). Propidium and its congeners are able to bind to various cellular and plasma proteins (4). It has been suggested, and some evidence exists, that drugs such as propidium iodide may bind to proteins that interact with either single- or double-stranded DNA, or that they bind to complexes of the two. In this way, they inhibit or perturb protein-nucleic acid interactions essential for such crucial cellular events as replication, transcription, or repair. Such a mechanism might then constitute an important component of the efficacy of the drug, that is, propidium could exert its cytotoxic effect by a mechanism other than intercalation into double-stranded DNA.

Propidium may bind to a purine- or pyrimidine-binding site on a DNA-binding protein. Douc-Rasy *et al.* (3) found that trypanocides closely related to propidium inhibit the catenating reaction of topoisomerases. The extreme dependence of trypanosomes upon topoisomerases as a consequence of their unusual kinetoplast DNA would render them especially sensitive to such inhibition. Filipski (5) proposed a model in which the drugs bind to a site on the topoisomerase which reversibly binds a nucleic acid base. The drugs compete with the bases and thereby interfere with the enzyme. Such a mechanism may be widespread for DNA-binding proteins and could explain the cytotoxic effects of many intercalating drugs.

In order to study propidium binding to a DNA-binding protein and a DNA-protein complex, X-ray diffraction methods were employed. The DNA-binding protein used was bovine pancreatic RNase A, an enzyme that preferentially binds single-stranded DNA and was the first DNA melting protein characterized (6, 7). It was co-crystallized in this laboratory with deoxytetraadenylate (8). Solution of the crystal structure by X-ray techniques showed that the resultant complex consisted of four tetramers of deoxyadenylate bound to each protein molecule (9). The details of the molecular associations are given elsewhere (10, 11).

Difference Fourier analysis was used in conjunction with molecular graphics to determine propidium-binding loci on the complex and to optimize molecular interactions. In addition, fluorescence spectroscopy was employed to assess drug binding to ribonuclease in solution. By these means, we were able to identify a previously unreported hydrophobic binding pocket adjacent to the enzyme catalytic site. Binding of propidium at this site perturbs catalytic residues. The solution binding studies corroborate these results and support propidium iodide as a competitive inhibitor of ribonuclease A. The findings lend some support to the hypothesis that the mechanism of action of this drug may be protein mediated.

Materials and Methods

Bovine pancreatic ribonuclease A (type 1-A) was purchased from Sigma and used for crystallization without further purification. Propi-

This research was supported by Grant GM-27838 from the United States Public Health Service.

ABBREVIATIONS: RNase, ribonuclease; $d(pA)_4$, deoxytetraadenylate; PEG, polyethylene glycol; d(CpA), deoxycytidylphosphoadenosine.

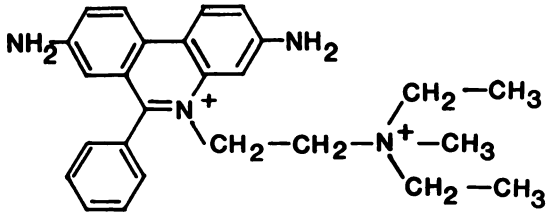

Fig. 1. Drawing of the structure of propidium iodide used in the studies presented here.

dium diiodide, uridine 3′-monophosphate, and adenosine 5′-triphosphate were also obtained through Sigma. Deoxytetraadenylate [d(pA)4] was purchased from Callaborative Research (Waltham, MA). The protein was dissolved in distilled water to approximately 20 mg/ml. The $d(pA)_4$ was also dissolved in distilled water. The relative concentrations in the crystal mother liquor maintained a molar stoichiometry of 5:1, nucleic acid to protein. Orthorhombic crystals of the complex having space group $P2_12_12_1$ were grown from polyethylene glycol (PEG) 4000. As previously described (8), these native crystals have cell dimensions of $a = 44.64$ Å, $b = 75.23$ Å, and $c = 44.72$ Å.

The crystals were treated with 1 mM solution of propidium iodide in PEG 4000 at a PEG concentration 5% higher than that used for crystallization, in order to enhance crystal stability (12). After approximately 10 days, the crystals assumed a deep purple color, whereas the background mother liquor had only a barely perceptible color. X-ray diffraction data were collected to 2.9 Å on an ADS multiwire area detector at the University of California, Los Angeles. The machine was operated at 40 kV × 120 mamp at a crystal-to-detector distance of 500 mm, and was equipped with a graphite monochromator. The data were collected at three different orientations: $X = 0$, oscillation of ϕ from 0 to 180; $X = 90$, oscillation of ω from +35 to −35; and $X = 20$, oscillation of ω from +35 to −35. X-ray diffraction data were also collected to 2.9 Å on an Enraf-Nonius CAD4 automated diffractometer as previously described for the native structure (8). For both diffractometer and multiwire data the integrated intensities were corrected for Lorentz and polarization effects as well as crystal absorption. The backgrounds were determined by nearest neighbor averaging of 27 reflections and subtracted, and the intensities were merged and converted to structure amplitudes. Structure amplitudes were scaled to equivalent native amplitudes [native being the ribonuclease plus $d(pA)_4$ complex] using a Fourier-Bessel procedure written by L. Weissman (University of California, Los Angeles) and modified by D. C. and R. W. All structure factor amplitudes with a magnitude <3 times their estimated standard deviation (constituting approximately 15% of the total data) were discarded. Other details of data processing can be found in Ref. 11.

Difference Fourier syntheses were computed to locate propidium iodide-binding sites. Difference coefficients between the native and derivative structures ($|F_{O\text{-}PROP} - F_{O\text{-}NAT}|$) were computed and combined with phases calculated from the refined native structure (11). The program FFT (written by R. Fisher) was used to calculate the fast Fourier transform, and PTXCONTUR, a program also written by R. F., was used to contour difference maps to facilitate visual inspection of electron density. Because the electron density maps generated in these experiments were difference Fourier maps, positive density should, in principle, represent bound drug molecules. Negative density coupled with positive density might represent alterations in local protein conformation induced by drug binding. To relate the difference density to the native unit cell contents, the coordinates for the protein and DNA were plotted as a series of two-dimensional sections. The sections were copied onto acetate sheets and these were superimposed on the corresponding sections of the difference electron density map. Peaks were considered in terms of magnitude, shape, and electrostatic and stereochemical consistency with the protein environment.

Molecular graphics on an Evans and Sutherland PS-300 system was used to fit the propidium iodide molecule to density. The structure of propidium iodide used in this analysis was generated from transformed coordinates for a published structure of ethidium (13) to the unit cell described above and positioned in electron density. The diethylmethylamine moiety was added to ethidium (to make propidium) using FRODO, a graphics program written by T. A. Jones (14) and run on the PS-300. Propidium was also fitted to the density using FRODO. The preliminary model was subjected to constrained-restrained least squares refinement using CORELS, written by J. L. Sussman (15). Initially, the program was used for rigid body refinement of protein, DNA, and drugs. This was then followed by dihedral angle refinement of protein and DNA. The progress of refinement was monitored periodically by examination on the molecular graphics system. Some torsional angles in the protein and in propidium were manually adjusted during the course of refinement to mitigate unfavorable ribonuclease-propidium contacts.

The distribution of conventional R factors for the refined model was not significantly different from that seen for the native RNase A + $d(pA)_4$ complex alone (11), and it appeared that the many small changes observed in the difference Fourier maps were adequately accommodated. Similarly, restraints were maintained throughout the refinement to values that yielded agreement with ideal geometry nearly the same as for the native structure.

Binding titrations, monitored by fluorescence spectroscopy, were carried out on a Perkin-Elmer MFP-66 fluorescence spectrophotometer interfaced with a Perkin-Elmer 7300 computer, which corrected for lamp fluctuations. Titrations were carried out in 1-cm cuvettes using a four-sample, turetted cuvette holder which enabled nearly simultaneous measurement of blank samples and instrument fluctuations. Excitation and emission wavelengths were 517 and 635 nm, respectively. Binding titrations were performed by monitoring either the changes in fluorescence or polarized emission associated with propidium iodide binding. Ribonuclease A, in 100 mM $NaPO_4$, pH 5.7, was titrated into 100 μM propidium iodide also containing 100 mM $NaPO_4$, pH 5.7. These titrations were repeated in the presence and absence of several concentrations of ATP, dATP, d(CpA) or 3′-UMP. It was necessary to titrate the ribonuclease into an invariant and somewhat low concentration of propidium because of the large inner filter effect associated with the chromophoric drug. Attempts to numerically correct for the effect, which obstructs incident light from reaching part of the sample, were unsatisfactory. A constant propidium concentration of 100 μM during the titration circumvented the problem. Equilibrium propidium iodide binding was monitored also by steady state fluorescence polarization. Vertical and horizontal components of the excitation and emission beams were resolved with dichroic sheet polarizers. Fluorescence polarization, P, was calculated from:

$$P = \frac{I(vv) - G^*I(vh)}{I(vv) + G^*I(vh)}$$

where I is the fluorescence intensity,

$$G = \frac{I(hv)}{I(hh)}$$

and the first and second subscripts refer to the vertical or horizontal orientation of polarization of excitation and emission beams, respectively. The factor G corrects for inequivalent transmittance of polarized light.

Results

X-Ray diffraction studies. The unit cell dimensions of the propidium-perfused crystals as determined by diffractometry were $a = 44.40$ Å, $b = 75.53$ Å, $c = 43.68$ Å. R_{SYM}, which is an indication of the accuracy of data collection, was calculated as follows:

$$R_{SYM} = \sum_{hkl} \| F_{hkl}| - |F_{hkl} \| / \sum_{hkl} [|F_{hkl}| + |F_{hkl}|]/2$$

and found to be 3.5% for the diffractometer data and 7.9% for

the multiwire data. Two measurements of each reflection were recorded on the diffractometer, while four to six were collected by the multiwire detector technique. Comparison of the propidium-derivatized crystal with the native produced a conventional R factor of 17.9% and 24% for the diffractometer and multiwire data, respectively, where

$$R = \sum_{hkl} \| F_{hkl-nat}| - K|F_{hkl-PROP} \| / \sum_{hkl} |F_{hkl-nat}$$

Difference Fourier maps were calculated and displayed using the diffractometer and multiwire data sets separately, and a third map was computed using the merged data. As far as the strongest feature on the maps was concerned, there were no significant differences. Examination of any one of the three difference Fourier maps revealed the presence of an exceptionally strong peak of electron density centered at 0.82, 0.08, and 0.70 in the unit cell. The height of the peak was substantially greater than the background value and the statistical probability of chance occurrence was approximately 1 in 100. The difference electron density, seen in Fig. 2, actually consists of three discrete lobes of differing sizes. The distinct tripartite shape of the difference electron density suggested the orientation and guided the fitting of the propidium molecule (which has three structural domains). Only minor adjustments in propidium's side chain torsional angles were required to position the three components of the drug within the difference electron density peaks.

The propidium was bound in a shallow hydrophobic depression on the protein with nearest neighboring residues Leu 51, Ala 52, Val 54, Phe 8, Met 13, Glu 49, and Gln 55. The pocket lies on the back side of the protein from the active center in the region formed by the segment 46–55, which is well fixed, and the poorly defined loop of polypeptide comprised of residues 13–18. The flexible segment 113–117 is also near by. The bound propidium is shown in Fig. 3, superimposed upon a skeletal structure of the RNase A molecule. This locus, to our knowledge, has not previously been observed to be a binding site on RNase A for any ligand.

Fig. 4 shows the RNase A structure in the immediate neighborhood of propidium. The difference density peak produced by propidium was in contact with several adjacent amino acid residues, and it was clear upon fitting that a molecule of the drug could not simply be inserted into the native protein without producing violations of van der Waals' distance constraints. Thus, it was necessary to adjust the amino acid side chains on the segment 46–55 and on the segment 13–18. Also, because of the flexible nature of the latter segment of polypeptide, it was not thought unreasonable to allow some small movements of the main chain as well. One residue that appeared to be a particular obstruction was Leu 51, whose alkyl side chain approached and interpenetrated the drug unreasonably if the native structure was assumed. Since Leu 61 was not well defined in the native RNase structure (16), especially at the terminal fork, it is probably mobile.

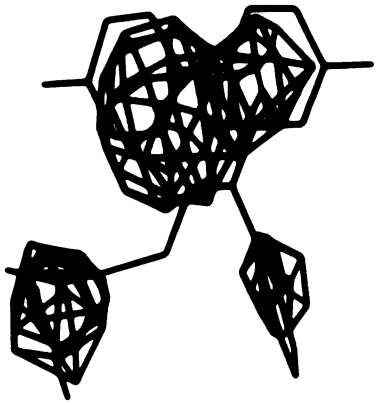

Fig. 2. Propidium iodide structure superimposed on the tripartite electron density appearing in the difference Fourier synthesis.

Two interactions which may be relevant to the binding of the propidium molecule involve the aromatic propidium chromophore, and Met 13 and Phe 8. These are both well positioned near-neighbors. The orientation of these residues, with respect to propidium, are shown in Figs. 5 and 6. Interatomic distances of 2.5–4.0 Å suggest that stabilization of drug binding may be enhanced by contact with these residues.

Inspection of the difference Fourier maps indicated that small alterations in the RNase + $d(pA)_4$ complex did occur as a consequence of the binding of propidium in the crystal. Regions of positive and negative density were observed in the neighborhood of both protein and DNA, and it was clear that some perturbation of structure occurred in addition to the changes in the immediate vicinity of the bound drug. These changes, although ubiquitous, were generally not large in magnitude. One exception to this, however, was the protein structure which bridged the 10 Å or so between the propidium-binding site and the active site residues of the enzyme. It was clear from the difference Fourier map that binding of propidium to RNase A generated conformational changes in the structure that were communicated to the active site by subtle movements in the intervening residues. These included, principally, the segment of polypeptide between residues 43 and 48, and the segment between residues 12 and 18. Thus, even though the propidium site is removed from the active site, it does appear to exert an effect on its constituent amino acids through linked conformational changes.

Fluorescence Spectroscopy. Preliminary examination of fluorescence excitation and emission spectra indicated an increase in the fluorescence intensity of propidium when in the presence of RNase A. Since RNase has no tryptophan and has no tyrosine residues in environments conducive to fluorescence, the protein has no intrinsic fluorescence. Titration of RNase into 100 μM propidium, as shown in Fig. 7a, produced a hyperbolic binding curve which inflected positively at higher protein concentrations. This suggested the presence of at least two classes of binding sites, one of high affinity and at least one significantly weaker. The K_d for the higher affinity binding site was calculated to be 1.1 mM.

In order to determine whether the tight binding site was located at the catalytic site of the enzyme (or proximal to it, such that propidium would act as a competitive inhibitor when bound), binding titrations were carried out in the presence of ATP, a competitive inhibitor of RNase which has a K_i of 4.0 mM (17). The results, which are shown in Fig. 7b, indicate that ATP does reduce the affinity of RNase for propidium. Experiments with dATP, also shown in Fig. 7b, yield similar results. If it is assumed that the reduction in binding affinity results from a competition between the nucleotides and propidium for the same site or for interacting sites, then the K_d observed for the inhibition should be: K_d observed = K_d actual * (1 + [I]/K_i). Using the inhibition data from Fig. 7, a and b, a value of

Figs. 3–5

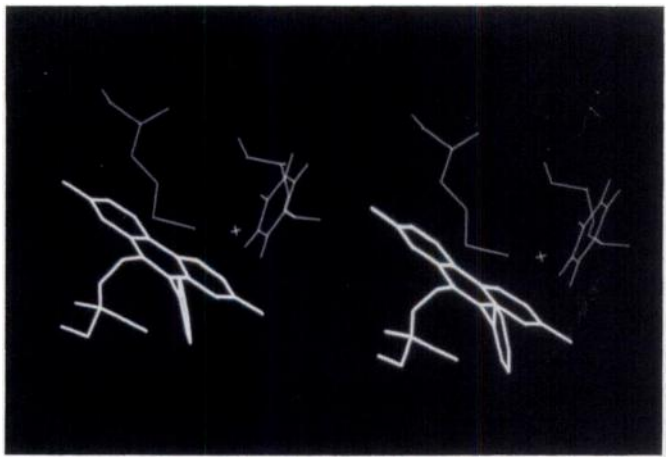

Fig. 6. The constellation formed by propidium with methionine 13 and phenylalanine 8.

1.2 mM was obtained. Since this is in close agreement with the measured dissociation constant of 1.1 mM, a competitive nature for the inhibition seems a reasonable assumption.

Fluorescence polarization was also used to assay for binding of propidium to the RNase A + $d(pA)_4$ complex. Fig. 7c shows that the polarization of propidium is increased in the presence of RNase, consistent with the drug molecule becoming fixed to the larger protein molecule. In the presence of the inhibitor, d(CpA), the polarization is significantly less, as would be expected if propidium were a competitive inhibitor of the enzyme.

A final fluorescence binding titration was conducted to more precisely delineate the nature of the propidium-binding site. Propidium demonstrated apparent competition with ATP, which occupies the outermost of the two binding sites in the RNase catalytic cleft (18), as well as the phosphate site at the catalytic center. In the nomenclature of Richards and Wyckoff (16), these are the A site and the P site. The experiment was repeated using 3′-UMP as the inhibitor to examine its ability to compete with propidium. The results, shown in Fig. 7d, show that 3′-UMP, which binds at the inner binding site (the B1 site) on the enzyme as well as the phosphate site at the catalytic center (the P site) (18, 19), does not reduce propidium binding to RNase. Inhibition, therefore, seems to result from competition by the drug for an intact A site. This is also consistent with the difference electron density map which shows changes in protein conformation primarily at the A site as a consequence of propidium binding.

Discussion

There are two significant conclusions that emerge from the crystallographic and fluorescence results we describe here. First, the crystalline RNase plus $d(pA)_4$ complex used in the X-ray studies presents to the propidium iodide an array of potential binding sites on both protein and DNA. The single-stranded DNA, in particular, with numerous extended and stacked bases in a variety of environments and conformations, offers many opportunities for interaction with propidium, a molecule known for its affinity for both single- and double-stranded DNA. Yet, the major site of binding, significantly stronger than any other, is not on the DNA but on the RNase.

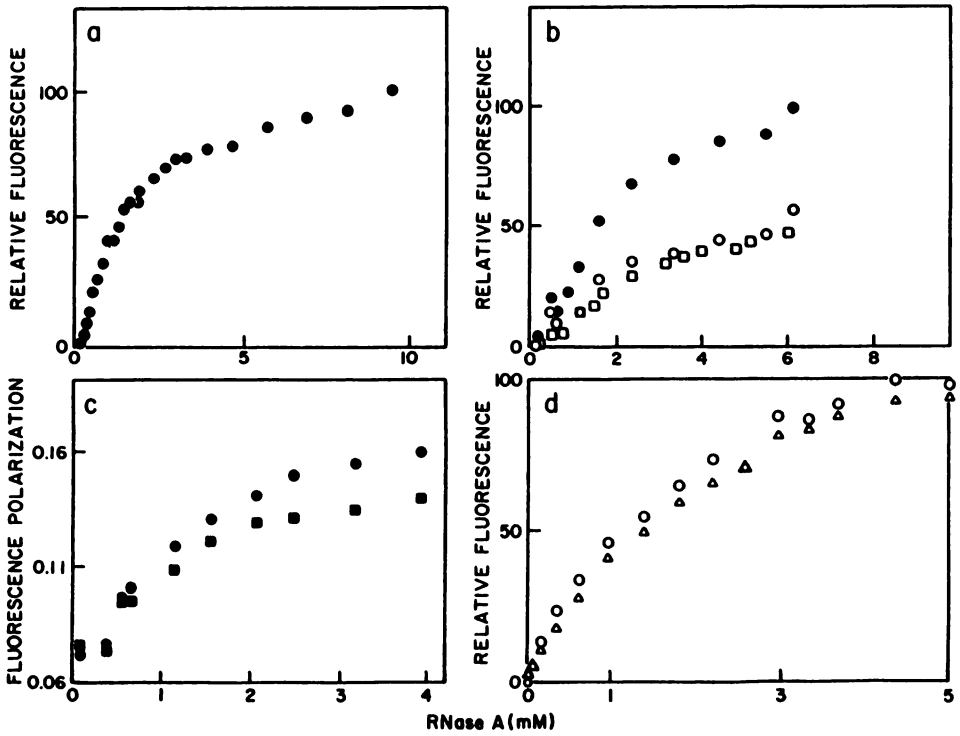

Fig. 7. a. The change in fluorescence upon titration of RNase A into a 100 μM solution of propidium iodide. The protein concentration was varied from 0 to 10 mM. Excitation wavelength was 517 nm and fluorescence emission was recorded at 635 nm. b. The change in fluorescence when 0–6 mM RNase A was titrated into a 100 mM propidium iodide solution in the absence (●) and presence (○) of 1.0 mM ATP, a competitive inhibitor of the enzyme, or (□) 10 mM dATP. c. The fluorescence polarization change upon titration of a 100 μM propidium iodide solution with RNase A in the absence (●) and presence (■) of d(CpA). d. The change in fluorescence as the same propidium iodide solution was titrated with RNase A in the absence (●) and presence (▲) of 4 mM 3′UMP. The protein concentration varied here from 0 to 5 mM.

Figs. 3 to 5. *Fig. 3.* The propidium molecule with an associated 1.5-Å surface is shown here in stereo superimposed upon the structure of RNase A. The drug occupies a shallow depression on the side of the protein molecule away from the active site cleft. This and other stereographic photos were generated by an Evans and Sutherland PS300 color graphics system. *Fig. 4.* A detail of the propidium iodide molecule superimposed on the surrounding protein structure is shown in stereo. *Fig. 5.* A stereo computer-generated image of a detail of the propidium iodide bound to RNase A with Met 13 and Phe 8, the closest residues, emphasized for clarity. Contact distances suggest Met 13 and Phe 8 may be of particular importance in securing propidium to the protein surface.

Thus, it appears to us that these results tend to support the hypothesis that the action of this and similar drugs may be protein mediated; that the target molecule is not necessarily DNA but a protein or class of proteins. Because RNase is a protein that binds both single-stranded RNA and DNA, we might speculate that the target class is comprised of nucleic acid-interactive proteins.

The second important feature of these results is that RNase A possesses a reasonably high affinity site that can serve to bind propidium and, presumably, other intercalating drugs having similar structural features. Not only does this site exist, but the binding there of drugs produces subtle structural perturbations in the RNase molecule that disturb a primary component of the substrate-binding site at the catalytic center. The kinetic effect implies a competitive interaction between the drug site and the nucleoside site (the A site). The difference Fourier maps suggest that this occurs by perturbation of intervening protein structure.

Propidium occupies a hydrophobic pocket on the reverse side of the protein from the RNase active site (Figs. 2–4). The primary residues involved include Leu 51, Ala 52, Val 54, Phe 8, Met 13, Glu 49, and Gln 55. The molecular environment suggests that propidium's initial attraction to this site is probably due to negatively charged residues, particularly Glu 9 and Glu 49. The drug may then be trapped in the pocket by favorable hydrophobic associations. One apparent interaction is with the sulfur of Met 13. Associations between sulfur atoms and π-bonded atoms have been observed previously and may serve to stabilize protein folding (20). The attraction between sulfur and aromatic residues is approximately 5 times the usual van der Waals' attraction of −0.2 kcal/mol. Distances between the sulfur atom and the chromophoric ring atoms of propidium are within the acceptable range and indicate that some stabilization of propidium may be so derived.

Interaction seems likely, as well, between the propidium ring system and Phe 8. Burley and Petsko (21) studied aromatic-aromatic interactions in small proteins and concluded that this phenomenon was important for protein stabilization. Fig. 6 shows the overlapping surfaces of propidium and Phe 8. During refinement, the phenylalanine ring rotated to assume an orientation such that its plane formed a near -70° angle with that of propidium. The centroid ring separation for propidium and Phe 8 was calculated to be 4.6 Å. Burley and Petsko (21) had found 4.5–7.0 Å to be optimal for structure stabilization. They further suggested that the edge-face type of ring interactions could be important in drug-protein interactions; this may be one such example.

Binding of propidium to this hydrophobic site affects active site substrate binding. The difference electron density map indicated that DNA, which is associated with the catalytic cleft, was perturbed. Structure refinement implied changes in the disposition of active site, as well as other residues, which included, for example, the imidazole ring of His 12 which moved and rotated. The initial attraction and binding of propidium is likely due to electrostatic attraction between the positive charge on the drug and negative charges on the protein. However, stability of the complex is probably conferred by the hydrophobic contacts that include interaction with sulfur of Met 13 and the edge-to-face arrangement with Phe 8. The fluorescence intensity of the drug increases upon binding of protein consistent with the hydrophobic character of the site. Fluorescence measurements indicated that propidium inhibits RNase with a K_d value lower than that found for many classic inhibitors of the enzyme (17).

Acknowledgments

This research was supported by a grant (GM-27838) from the United States Public Health Service. The authors wish to thank Mr. Greg DeLozier for his valuable contributions and the Molecular Structure Group at UCLA for the use of their facilities.

References

1. Davidson, M. W., B. G. Griggs, I. G. Lopp, and W. D. Wilson. *Biochimm. Biophys. Acta* **479**:378 (1977).
2. Patel, D. J., and C. Shen. *Proc. Natl. Acad. Sci. USA* **75**:2553 (1978).
3. Douc-Rasy, S., A. Kayser, and G. F. Riou. *EMBO J.* **3**:11 (1984).
4. Tas, J., and G. Westerneng. *J. Histochem. Cytochem.* **29**:926 (1981).
5. Filipski, A. *FEBS Lett.* **159**:6 (1983).
6. Jensen, D. E., and P. H. von Hippel. *J. Biol. Chem.* **251**:7198–7214 (1976).
7. Record, M. T., T. M. Lohman, and P. de Haseth. *J. Mol. Biol.* **107**:145–158 (1976).
8. Brayer, G. D., and A. McPherson. *J. Biol. Chem.* **257**:3359–3361 (1981).
9. McPherson, A., G. D. Brayer, and R. Morrison. *Biophys. J.* **49**:209–219 (1986).
10. McPherson, A., G. Brayer, D. Cascio, and R. Williams. *Science (Wash. D. C.)* **232**:765.
11. McPherson, A., G. D. Brayer, and R. D. Morrison. *J. Mol. Biol.* **189**:305–328 (1986).
12. Cascio, D., R. Williams, and A. McPherson. *J. Appl. Crystallogr.* **17**:209–210 (1984).
13. Tsai, C. C., S. C. Jain, and H. M. Sobell. *J. Mol. Biol.* **114**:301 (1977).
14. Jones, T. A. In *Computational Crystallography* (D. Sayer, ed.). Oxford University Press, New York, 307–317 (1982).
15. Sussman, J. L., S. R. Holbrook, G. M. Church, and S. H. Kim. *Acta Crystallogr.* **A33**:800 (1977).
16. Richards, F. M., and H. W. Wyckoff. *Atlas of Molecular Structures in Biology.* Vol. 1: *Ribonuclease S.* Clarendon Press, Oxford (1973).
17. Walz, F. G. *Biochemistry* **10**:2156–2162 (1971).
18. Wodak, S., M. Y. Ieu, and H. W. Wyckoff. *J. Mol. Biol.* **116**:855–875 (1977).
19. Borkakoti, N. *FEBS Lett.* **162**:367–373 (1983).
20. Morgan, R. S., C. E. Tatsch, R. H. Gushard, J. M. McAdon, and P. K. Warme. *Int. J. Peptide Protein Res.* **11**:209 (1978).
21. Burley, S. K., and Petsko, G. A. *Science (Wash. D. C.)* **229**:23 (1985).

Send reprint requests to: Dr. Alexander McPherson, Department of Biochemistry, University of California, Riverside, CA 92521-0129.